COMPOSITION EFFECTS ON PHASE FORMATION AND STABILITY

Kenneth F. Kelton
Department of Physics
Washington University
St. Louis, MO 63130
USA
Phone - 314-935-6228
FAX - 314-935-6219
email: kfk@howdy.wustl.edu

INTRODUCTION

More rapid techniques for obtaining accurate values of temperature-dependent nucleation and growth rates are needed for materials development. Small changes in stability due to composition shifts or the introduction of heterogeneous nucleation agents could be assessed quickly and experiments could be carried out remotely, such as in a microgravity environment, where the data are often taken under conditions that preclude the possibility of multiple experiments for different times at different temperatures. Differential scanning calorimetry (DSC) and differential thermal analysis (DTA) are ideally suited for these cases, yielding estimates of phase transition temperatures and enthalpies of transformation. When coupled with microstructural studies they can also give information about the mode and kinetics of transformation. The low apparatus weight and the small samples required make DSC/DTA studies ideal for supporting investigations in a reduced gravity environment. Samples processed in space, for example, might be screened quickly allowing in-flight modifications of the processing parameters. DSC/DTA investigations often suffer, however, from the lack of quantitative methods for data analysis.

Under continuing NASA support within the Microgravity Division, we have developed realistic numerical models for DSC/DTA measurements of first order phase transformations proceeding with time-dependent nucleation and cluster-size-dependent growth rates [1-3]. Account was also taken of finite sample sizes, surface crystallization and heterogeneous nucleation [3,4]. These past studies have focused on polymorphic crystallization, where the compositions of the initial and final phases are identical. Since only a limited number of phase transformations are approximately polymorphic, we are extending the models to include nucleation and growth in primary crystallizing glasses and for precipitation processes. Though growth in such cases, involving solute redistribution, has been investigated extensively, the evaluation of time-dependent nucleation rates is less clear. Previous experimental studies of compositional effects on the steady-state nucleation rate are few and interpretations of the data are sometimes difficult. Further, there are no previous experimental measurements of the composition dependence of the time-dependent nucleation rates. These data are essential to guide the development of a model for nucleation that can be included in our numerical models of DSC/DTA peak profiles.

In this report, results from experimental studies of the composition dependence of nucleation are presented. A model for nucleation that takes simultaneous account of the interfacial attachment

processes at the growing cluster interface and diffusion into the region surrounding the developing cluster is presented and numerical results are discussed.

EXPERIMENTAL STUDIES OF COMPOSITION-DEPENDENT NUCLEATION

To guide the development of a model for nucleation in partitioning systems, experimental studies in metallic and silicate glasses and in undercooled liquid metals are underway.

a. Time-Dependent Nucleation Studies in $(Na_2O-2CaO)_{1-x}(3SiO_2)_x$ Glasses

Time-dependent nucleation rates were measured in as-quenched glasses of $Na_2O.2CaO.3SiO_2$ made with varying SiO_2 concentrations, using the two-step annealing method, for which nuclei are first produced at temperatures where growth is insignificant, and subsequently grown at higher temperatures where the nucleation rate is small [5]. The slope of the number of nuclei produced as a function of time is equal to the time-dependent nucleation rate, I(t). The induction time for nucleation, θ, is the intercept with the time axis of the portion of the graph where the number of nuclei increases linearly with time, corresponding to the steady-state nucleation rate, I^s.

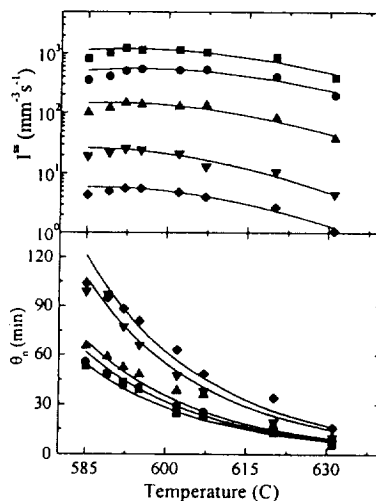Fig. 1. Crystal steady-state nucleation rates (top) and induction times (bottom) as a function of temperature for glasses of different composition: ■ - $[SiO_2]$ = 0.494; ● - $[SiO_2]$ = 0.5 (stoichiometric glass); ▲ - $[SiO_2]$ = 0.506; ▼ - $[SiO_2]$ = 0.52; ◆ - $[SiO_2]$ = 0.53. A growth anneal of 5 minutes at 700°C was used. The solid lines through the points are a fit to the steady-state nucleation rates assuming a composition-dependent interfacial energy. (From [5]).

The measured data are shown in Figure 1. To most easily indicate the amount of silica in the glass, compositions are written as $(Na_2O.2CaO)_{1-x}(3SiO_2)_x$; x=0.5 corresponds to the stoichiometric glass. The magnitudes of the steady-state nucleation rates decrease with increasing $[SiO_2]$ while the induction times increase. Changes in the growth velocity (not shown) scale inversely with changes in the induction time. The composition dependence of the nucleation rate cannot be explained by changes in the atomic mobility, as was suggested earlier by others [6], since I^s is a much stronger

382

function of the composition than is the induction time, which scales inversely with the mobility [7]. Further, measurements of the liquidus temperature demonstrate that changes in Γ^s do not arise from changes in the driving free energy for crystallization [5]. If the classical theory remains correct, then, the composition dependence of the time-dependent nucleation rate arises from changes in the interfacial free energy. Detailed modeling of the time-dependent nucleation rate using the kinetic model of the classical theory [5,8] confirm this.

b. Nucleation Studies in Metallic Glasses

Most Zr-based easy metallic glass formers and many Al-rare earth (Al-RE) glasses devitrify to nanostructured materials [9,10]. The density of crystallites indicates a very high nucleation rate, 10^{19} - $10^{21}/m^3$ s, that often saturates quickly, and a low growth rate, which is strongly size dependent [11]. Because solute partitioning is central to the crystallization of these glasses, their nucleation behavior is relevant to our investigations. We recently reported the first direct measurements of time-dependent nucleation in a metallic glass by the two-step annealing method for $Zr_{65}Al_{7.5}Ni_{10}Cu_{17.5}$ metallic glasses [12]. The tendency for phase separation occurring simultaneously with nucleation and growth in the Zr-based glasses, which may also give a high density of crystallites, however, complicates the data analysis. Though phase separation is unlikely in the Al-RE glasses, the large nucleation rate in the growth regime make two-step annealing studies difficult. To get round these difficulties, annealing-induced crystal-size distributions in Al-Y-Fe glasses are being measured, and other Al-RE glasses (e.g. Al-La and Al-Sm) are under study. Our initial measurements of the size distributions for α-Al in annealed Al-Y-Fe glasses are shown in fig. 2. The rise in the density of large clusters with decreasing size signals transient nucleation. Within measurement error, the peak cluster size is independent of the annealing temperature, though the peak density is larger for the glass annealed at the higher temperature. The density decreases for small clusters, signaling either a decrease in the homogeneous nucleation rate, or a saturation of heterogeneous sites. The high cluster density at both high and low annealing temperatures makes the latter explanation unlikely. Differential scanning calorimetry studies of these glasses will be used to refine extensions being made to models of calorimetric data.
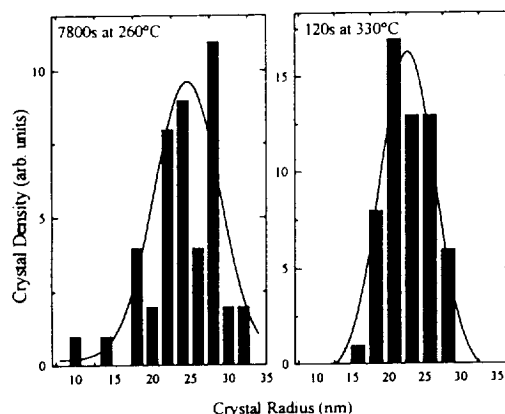

Fig. 2 - Crystal size distributions from annealed $Al_{88}Y_7Fe_5$ glass

c. Undercooling Studies in Ti-3d transition metal-Si-O alloys

Previous studies by us [13] and others [14] have shown that the interfacial energies between undercooled liquids or glasses, and quasicrystals or their crystal approximants (believed to have the same local structure as the related quasicrystal) are small. The nucleation rates, then, should depend strongly on the chemical compositions of the liquid and quasicrystal/crystal approximant. To investigate this, the microstructural evolution of undercooled Ti-Cr-Si-O, Ti-Mn-Si-O and Ti-Fe-Si-O liquids of the composition of the 1/1 crystal approximant to the icosahedral phase were studied using the NASA drop-tube facility at Marshall (in collaboration with T. Rathz and M. Robinson) and by rf-levitation at the DLR in Cologne (in collaboration with D. Holland-Moritz and D. Herlach). Although we have demonstrated that the 1/1 phase forms in all of these alloys, and is a stable phase in Ti-Cr-Si-O and Ti-Fe-Si-O, SEM backscattering studies of the solidification microstructures demonstrate that it only forms as the primary crystallizing phase in Ti-Fe-Si-O alloys. The α-Ti phase is the primary crystallizing phase in Ti-Cr-Si-O and Ti-Mn-Si-O phases.

Our determinations of the equilibrium phase diagram for Ti-Fe-Si-O show that 1/1 phases with composition $Ti_{67-71}Fe_{21-27}Si_{6-8}O_{4-10}$ are stable, forming directly from the liquid. The liquidus temperature, $T_m = 1255°C$, is lowest for $Ti_{68}Fe_{26}Si_6O_4$. For [Ti] < 67 at.%, only one Ti_2Fe (a=11.30 Å) phase forms with the 1/1 approximant. For [Ti] > 72 at.%, another Ti_2Fe phase with a smaller lattice constant (a=11.07 Å) forms in addition to these two phases. Below $\approx$ 1200°C the 1/1 phase decomposes to a phase mixture of the larger Ti_2Fe phase (a=11.30 Å) and Ti_5Si_3. Both the 1/1 and the Ti_2Fe phases, which contain strong local icosahedral order, show small undercoolings. Reduced undercooling values, $\Delta T_r = \Delta T/T_m$, obtained by levitation melting for the 1/1 phase lie between 0.11 and 0.12. As expected, the amount of undercooling increases as the composition is moved away from the stoichiometric value for the 1/1 phase.

These promising results and the small temperature range between the liquidus and the solidus near the 1/1 composition (75 to 100°C) indicate that this alloy might be a good candidate for a future space shuttle experiment, though the melting temperatures are high. Contactless measurements of the viscosity and specific heat would provide parameters needed for a quantitative analysis of the undercooling data.

NEW KINETIC MODEL FOR NUCLEATION IN PARTITIONING SYSTEMS

Experimental evidence from our glass devitrification studies [8], from precipitation processes [15] and for the devitrification of bulk metallic and Al-RE glasses [9-11] suggests that the classical theory of nucleation is inadequate in some cases to explain nucleation in partitioning systems. We have extended the classical theory of nucleation to take account of diffusion to lowest order, building upon a model proposed earlier by Russell [16]. The cluster distribution is a function of both the cluster size, n, and of the number of solute atoms in the nearest neighbor shell to the cluster, ρ. Cluster growth is based on the relative rates of exchange of solute atoms with the glass and with the cluster interior. The time-dependent nucleation rate is obtained from a numerical solution to the coupled differential equations that describe the time dependence of the cluster density, $N(n,\rho)$,

$$\frac{\partial N(n,\rho)}{\partial t} = \alpha(n,\rho-1)*N(n,\rho-1) - [\alpha(n,\rho) + \beta(n,\rho)]*N(n,\rho)$$

$$+\beta(n,\rho+1)*N(n,\rho+1) + k^+(n-1,\rho+1)*N(n-1,\rho+1)$$

$$+ k^-(n+1,\rho-1)*N(n+1,\rho-1) - [k^+(n,\rho) + k^-(n,\rho)]*N(n,\rho) \ .$$

Here α and β are, respectively, the rates at which atoms enter and leave the neighborhood of the cluster and k^+ and k^- are, respectively, the interfacial attachment and detachment rates. If the solute concentration in the parent phase is high, the depletion of solute near the interface with cluster growth will be less than expected, since after atom incorporation the cluster interface moves into the neighboring region. For the discussion presented here, this complication is ignored. When the diffusive fluxes are linked with the interfacial processes underlying cluster growth an excess solute concentration in the neighborhood of sub-critical clusters can develop. This results because sub-critical clusters are on average dissolving. Atoms that diffuse to the neighborhood of those cluster interfaces tend to remain there. This is demonstrated in fig. 3, using parameters appropriate for oxygen precipitation in silicon [17]. Calculations show that the scaling behavior for I/I^s with t/θ is the same as from the classical theory of nucleation. I^s and θ are intermediate between the values for interface and diffusion limited nucleation in the classical theory.
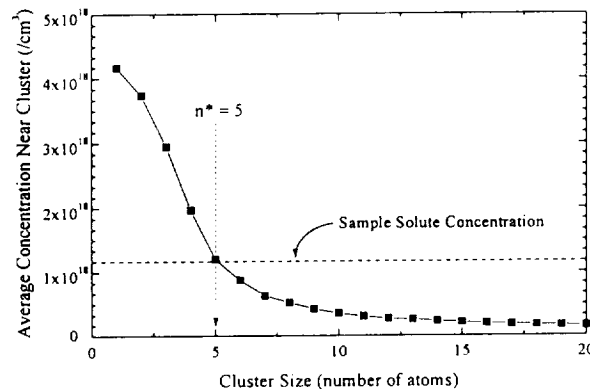

Fig. 3 - Computed average concentration of solute atoms in the neighborhood of clusters of different size. Computed for oxygen precipitation in Czochralski-grown silicon assuming an interfacial free energy of 0.38 J/m^3 and using accepted parameters [15]. The critical size, n*, at the annealing temperature is indicated.

The nucleation features in bulk metallic glasses are explained within this new model [17]. A significant population of small clusters exists in quenched glasses [3,18,19] For glasses that partition upon crystallization, those clusters are surrounded by an enhanced solute concentration. Since calculated and experimental data for polymorphic glasses demonstrate that a higher temperature distribution is retained due to kinetic freezing during the quench, clusters that are even larger than the critical size at the annealing temperature will be surrounded by a matrix rich in

solute, due to the larger critical sizes at the higher temperatures. When the glasses are annealed, these clusters will grow quickly until the nearby excess solute is consumed. As is experimentally observed [11], growth will then abruptly slow down, limited subsequently by long-range diffusion. Due to the large population of small clusters, this scenario results in the high density of small crystallites. It also explains why the rate of nuclei generation drops significantly with annealing time.

REFERENCES

1. K.F. Kelton, J. Am. Ceram. Soc., **75**, 2449 (1992).
2. K. F. Kelton, J. Non-Cryst. Solids, **163**, 283 (1993).
3. K. F. Kelton, K. L. Narayan, L. E. Levine, T. C. Cull and C. S. Ray, J. Non-Cryst. Solids, **204**, 13 (1996).
4. K. Lakshmi Narayan, K. F. Kelton and C. S. Ray, J. Non-Cryst. Solids, **195**, 148 (1996).
5. K. Lakshmi Narayan and K.F. Kelton, J. Non-Cryst. Solids, **220**, 222 (1997).
6. P. F. James, in: Glasses and Glass Ceramics, ed. M. H. Lewis (Chapman and Hall, London, 1989). p. 80.
7. K. F. Kelton, in Solid State Physics, Vol. 45, ed. H. Ehrenreich and D. Turnbull (Academic Press, Boston, 1991), p. 75.
8. K. Lakshmi Narayan and K. F. Kelton, Acta Mat. (in press).
9. R. Busch, S. Schneider, A. Pecker and W. L. Johnson, Appl. Phys. Lett., **67**, 1544 (1995).
10. J. C. Foley, D. R. Allen and J. H. Perepezko, Scripta Materialia, **35**, 655 (1966).
11. M. Calin and U. Köster, Proceedings of ISMANAM-97, held in Barcelona, Spain (1997).
12. T. K. Croat and K. F. Kelton, MRS Proceedings, Symposium B, Boston, MA (1997).
13. J. C. Holzer and K. F. Kelton, Acta Metall. Mater., **9**, 1833 (1991).
14. D. Holland-Moritz, D. M. Herlach and K. Urban, Phys. Rev. Lett., **71**, 1196 (1993).
15. K. F. Kelton and R. J. Falster, MRS Symposium Proceedings, San Francisco, CA (1997).
16. K. C. Russell, Acta Metall., **16**, 761 (1968).
17. K. F. Kelton, Phil. Mag. Lett., **77**, 337 (1998).
18. A. L. Greer, Acta Metall., **30**, 171 (1982)
19. K. F. Kelton and A. L. Greer, J. Non-Cryst. Solids, **79**, 295 (1986).